GLOBAL WAVE CLIMATE TREND AND VARIABILITY ANALYSIS

Sofia Caires
Meteorological Service of Canada and Royal Netherlands Meteorological Institute
P.O. Box 201, NL-3730 AE De Bilt, Netherlands
email: caires@knmi.nl

Val Swail
Meteorological Service of Canada, Toronto, Ontario, Canada

1. INTRODUCTION

In a series of works, Wang and Swail (2001, 2002, 2004) have provided the scientific and the ocean and offshore engineering communities with seasonal trends and patterns of variability of significant wave height (H_S) in the Northern Hemisphere during the last 40 years in terms of means, 90th and 99th percentiles, and return value estimates. Their studies were based on two 6-hourly reanalyses data sets, covering the 1958-1997 period.

The first data set, the Cox and Swail (2001) reanalysis, produced wave fields on a global 1.25º x 2.5º latitude/longitude grid, and was obtained by using the reanalysis winds from American National Center for Environmental Prediction and the National Centers for Atmospheric Research (NCEP/NCAR) (Kalnay et al., 1996) to force the second generation ODGP2 spectral ocean wave model (see Cox and Swail, 2001).

The second, the Swail and Cox (2001) reanalysis, produced wave fields on a 0.625º x 0.833º latitude/longitude grid covering the North Atlantic. It was motivated by deficiencies in the NCEP/NCAR reanalysis winds, which led the authors to carry out an intensive kinematic reanalysis of the NCEP/NCAR surface wind fields and use the resulting improved winds to force the OWI 3-G wave model (see appendix of Wang and Swail (2002) and references therein).

More recently, another wave reanalysis data set on a global 1.5º x 1.5º latitude/longitude grid covering the period of 1957 to 2001 has been made available - the ERA-40 dataset. This reanalysis was carried out by the European Centre for Medium-Range Weather Forecasts (ECMWF), using its Integrated Forecasting System, a coupled atmosphere-wave model with variational data assimilation. A distinguishing feature of ECMWF's model is its coupling, through the wave height dependent Charnock parameter (see Janssen et al., 2002), to a third generation wave model, the well-known WAM (Komen et al., 1994), which makes wave data a natural output of ERA-40. A large subset of the complete ERA-40 data set, including H_S, can be freely downloaded and used for scientific purposes from the website http://data.ecmwf.int/data/.

The results of ERA-40 have been extensively validated against observations (Caires and Sterl, 2005) and other reanalysis data sets (Caires et al., 2004a). These studies concluded that the ERA-40 data set, although severely underestimating high sea states, compares better with the observations in terms of root mean square error and scatter index than the Cox and Swail (2001) data set, and that the Swail and Cox (2000) data set is the best in describing synoptic wave data in the North Atlantic. In terms of long-term variability, the different reanalysis wave data sets differ mainly in the Tropics and, as regards the period before 1981, in the Southern Hemisphere. Besides the underestimation of high percentiles, the ERA-40 data set has another limitation that seriously discourages its use in direct studies of climate variability and trends: the existence of inhomogeneities in time due to the assimilation of different altimeter H_S data sets in the ERA-40 computations (see top panel of Figure 1).

These two limitations in the ERA-40 H_S data set motivated their correction by Caires and Sterl (2005). These authors corrected the data using a nonparametric regression method, the main idea of which was to estimate the expected error between ERA-40 H_S and "true" H_S conditional on past (up to 12 hours) and present values of the former, using data from locations at which both ERA-40 and Topex measurements were simultaneously available, and then to use this conditional expected value to correct the whole ERA-40 data. The result was a new 45-year global 6-hourly dataset - the C-ERA40 dataset. Comparisons of the C-

ERA40 data with measurements from in-situ buoy and global altimeter data show clear improvements in both bias, scatter and percentiles in the whole range of values and the removal of the inhomogeneities present in the ERA-40 dataset. This data set can also be freely obtained for scientific purposes from the authors.

Caires et al. (2004b) used the ERA-40 global wind speed, H_S and mean wave period data, and the C-ERA40 H_S data, to create a global wave climatologic atlas available at http://www.knmi.nl/waveatlas, which gives a complete picture of the global wave climate and variability. The statistics presented in the atlas are, however, based on monthly, annual or decadal data, and therefore do not allow a direct comparison with those obtained in the works of Wang and Swail.

The main objective of the present study is to infer from the C-ERA40 seasonal trends in the mean, high percentiles and return value estimates of H_S, and to compare the results with those of Swail and Wang (2001, 2002, 2004), which were based on the Swail and Cox (2000) and on the Cox and Swail (2001) reanalysis datasets. Besides this, we will present *global* results (not restricted to the Northern hemisphere, like those of Wang and Swail), and comparisons between the trends inferred here from the C-ERA40 data set and the trends obtained for different sub periods of the last four decades by Carter and Draper (1988), Bacon and Carter (1991), Bouws et al. (1996) and Günther et al. (1998) in specific locations or small regions in the North Atlantic, by Allan and Komar (2000) and Gower (2002) in some buoy locations in the North Pacific, and by Sterl et al. (1998) globally. Wang and Swail (2002) also provide trend estimates homologous to those of most of these studies based on the reanalysis data sets used by them.

In our analysis we will not consider the ERA-40 dataset because of the above mentioned inhomogeneities in its H_S data set. The main inhomogeneity occurs from 12-1991 to 05-1993 and is due to the assimilation of faulty ERS-1 FDP (Fast Delivery Product) wave height data; it can be easily seen in Figure 1, which presents the time series of globally averaged monthly means, 90th and 99th percentiles of ERA-40 and C-ERA40 H_S. The inhomogeneity is most prominent for the monthly means, but it is equally present in the high percentiles. As can be verified in Figure 1, the C-ERA40 data set is free from this problem. For comparisons between trends in the ERA-40 and C-ERA40 data sets the reader is directed to the above mentioned global wave climatologic atlas (http://www.knmi.nl/waveatlas).

The paper is organized as follows: We start by describing our methods of analysis in Section 2. In the following three sections we present and comment the results of trend, extreme value and variability analyses. Finally, in Section 6 we summarize our main conclusions.

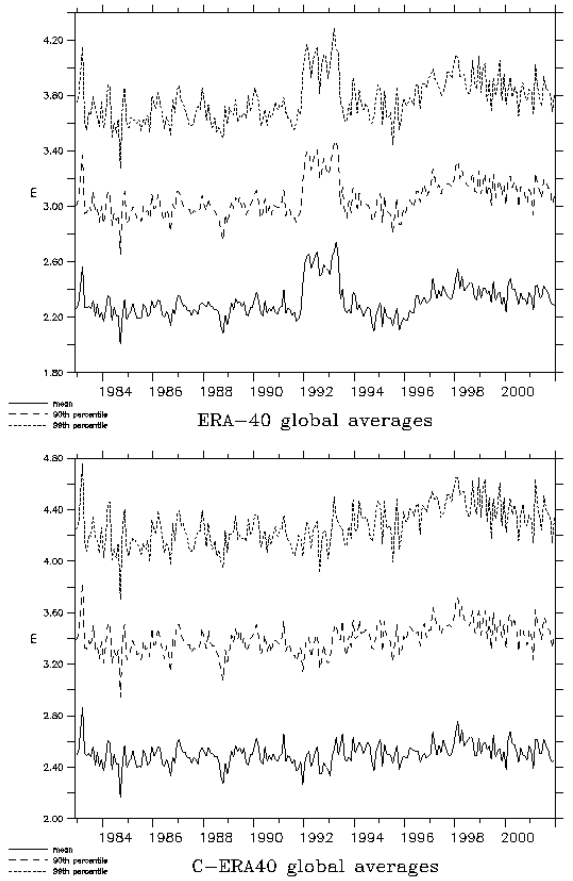

Figure 1. Time series of globally averaged H_S monthly means, 90th and 99th percentiles computed from ERA-40 (top panel) and C-ERA4 (bottom panel) 6-hourly fields.

2. METHODS OF ANALYSIS

We have mostly tried to analyse the data as Wang and Swail did. In the analysis of both trends and patterns of variability we will be using exactly the same techniques they did. In the analysis of trends in extreme values we will use a different but theoretically equivalent model that in principle - because it uses more data under essentially the same assumptions - allows better estimates. Our methods are succinctly described in the following subsections; except perhaps for the subsection on non-stationary methods of extremes (which contains some details), their purpose is merely to inform the reader of exactly what tools we use, so for theoretical background and detailed motivation the reader should resort to the references given.

2.1 TRENDS

Throughout, we use the term "trend" to mean the slope of the linear relationship between a variable being considered and time.

The trend analysis was carried out in the way described by Wang and Swail (2001, 2002). The Mann-Kendall non-parametric test for randomness against trend (Mann (1945) and Kendall (1955)) was used to identify the statistically significant trends at a 5% level, and the trend estimator is based on Kendall's rank correlation (Sen, 1968). Since the results of the Mann-Kendall test depend on autocorrelation, the effects of autocorrelation were also taken into account by pre-whitening those series for which the autocorrelation at lag 1 is higher than 0.05 (see Appendix A of Wang and Swail (2001) for details).

2.2 EXTREME VALUES

In order to assess changes in terms of distribution of extremes of wave height, Wang and Swail (2004) fitted the non-stationary Generalized Extreme Value distribution (GEV; see e.g. Coles (2001)) to annual maxima of H_S and investigated the existence of trends in the location or scale parameter of the distribution. They found that the only significant trends occurred in the scale parameter, and subsequently fitted a non-stationary GEV model with a linear trend in the location parameter and fixed scale and shape parameters to seasonal maxima of H_S from 1958 to 1997.

One of the currently most used methods in extreme value analyses in the stationary setting is the peaks-over-threshold (POT) method, in which the occurrence of 'storms' above a certain threshold and the magnitude of peak observations from 'independent' storms are modeled with Poisson and Generalized Pareto (GPD) distributions, respectively (see e.g. Coles (2001) or Caires and Sterl (2005b)). The older and equally sound annual maxima (AM) method, in which the GEV distribution is fitted to seasonal maxima, is also frequently used, but it tends to be somewhat wasteful in data; for example, in a typical application to 40-years of data, the annual maxima approach will yield only 40 data points. For this reason, and especially when the purpose is to obtain as accurate as possible inferences about the parameters governing extremes, the POT/GPD approach is often preferable to the AM/GEV approach.

In the non-stationary setting this seems to be even more the case, since then we are dealing with an even larger number of parameters. Therefore, in this work we will use the non-stationary analogue of the POT/GPD approach, which is based on the non-homogeneous Poisson process (NPP), to study the existence of, and to estimate, trends in the extremes of C-ERA40 data. Asymptotically, or theoretically, our results should be the same as those obtained using a non-stationary GEV, but because we are dealing with short time series it is important to take advantage of less data wasteful techniques.

In the point process approach to modelling extreme values (see Smith (1989), Anderson et al. (2001) and Coles (2001) for details), one looks at the times at which "high values" occur and at their magnitude. If t denotes the generic time at which a high value occurs and x is the corresponding magnitude of the variable of interest, then the point process consists of a collection of points (t, x) in a region of the positive quadrant of the plane. In practice, such a collection of points has first to be extracted from the original time series in such a way that the x components can be modeled as independent random variables. The way this is usually done with wave and similar data is by a process of "declustering" in which only the peak exceedences (highest observations) in clusters of successive exceedances ('storms') of a specified threshold or level are retained and, of these, only those which in some sense are sufficiently apart (so that they belong to more or less "independent storms") will be considered as belonging to the collection of points of the point process. The process of declustering is thus based on fixing a threshold over which one can consider exceedances and hence define the cluster peaks.

Thus our point process, or rather its "realization", consists of a collection of points belonging to the plane set $C = \{(t, x) : x > u(t), 0 \le t \le T\}$ where T is the number of years (in our case) over which observations are available and $u(t)$ denotes the threshold at time t. The non-homogeneous Poisson process (NPP) model of extremes is specified by the following two properties. Firstly, if A is a subset of C, then the number of points occurring in A, which we denote by N(A) is a random variable with a Poisson probability function with mean $\rho(A)$, where, writing $x_+ = \max(0, x)$ for real x,

$$\rho(A) = \int_A \lambda(t, x) dt\, dx ,$$

$$\lambda(t,x)=\frac{1}{\sigma(t)}\left(1+\xi(t)\frac{x-\mu(t)}{\sigma(t)}\right)_{+}^{-\frac{1}{\xi(t)}-1} \quad \text{for } (t,x)\in C,$$

and $\mu(t)$, $\sigma(t)$ and $\xi(t)$ are respectively the *location, scale and shape parameters* - or rather "parameter functions" - that may depend on time and need to be specified and estimated in practice.

The *m*-year return value, x_m, is determined by solving

$$\int_0^m \left(1+\xi(t)\frac{x_m-\mu(t)}{\sigma(t)}\right)^{-\frac{1}{\xi(t)}} dt = 1.$$

In the specific case presented here, all the parameters of the NPP model will be kept constant, apart from the location parameter; i.e., we will consider the model $NPP\,(\mu=\alpha+\beta t,\sigma,\xi)$ where t is time in years: $t=1,2,...,T$.

The threshold $u(t)$ is also taken constant, and so data sampling will follow the usual POT approach. The threshold will be defined as the 97th percentile of the empirical distribution of the 6-hourly ERA-40 H_S series. This specification is based on previous studies with the stationary approach (Caires and Sterl, 2005b), where it was found that the 97th percentile provided a reasonable threshold value (over which the asymptotic models of extreme value theory were thought to provide a good approximation).

The peak exceedances and the times at which they occur are represented by $\{t_{i,j}, x_{i,j}\}$, $j=1,2,...,n_i$, $i=1,2,...,T$, where n_i is the number of clusters in the *i*-th year . They correspond to the peaks of cluster exceedences above the threshold u and the times at which they occur obtained from the 6-hourly time series of the reanalysis data. The declustering method we use in order to arrive at this sample is the usual one of identifying clusters and picking their maxima and times where they occur except that we have taken care in treating cluster maxima at a distance of less than 48 h apart as belonging to the same cluster (storm) and hence collecting only the highest of the two.

The parameters of the NPP model outlined above were estimated by the maximum likelihood method (Smith (1989) and Anderson et al. (2001)); the maximization was carried out numerically using the Downhill Simplex Method (Press et al., 1992).

In order to assess whether the trends in the location parameter are statistically significant, we use the likelihood ratio test (Coles, 2001) to compare the NPP with a trend in the location parameter with the NPP with all parameters constant.

2.3 VARIABILITY MODES

We have used standard principal components or empirical orthogonal function (EOF) analysis (Preisendorfer, 1988) to obtain main modes of variability, in order to investigate whether they are linked to known dynamic mechanisms.

3. TREND ANALYSIS

There are many published works reporting trends in H_S in the last 5 decades in the North Atlantic. Carter and Draper (1988) and subsequently Bacon and Carter (1991) reported increases of 3.4 cm/yr and 2.2 cm/yr, respectively, in the annual means of observations from the Seven Stones light vessel (SSLV). Bouws et al. (1996) reported increases in the mean H_S 50th percentile in a 5°x10° lat/long box in the Northwest Atlantic of 2.3 cm/yr and of 2.7 cm/yr for a same size box in the Northeast Atlantic. Günther et al. (1998) report several rates of changes in the annual mean, 90th and 99th percentiles and annual maxima of H_S in the North Atlantic. Wang and Swail (2002) have compared the trend estimates obtained from the Swail and Cox (2000) data set with those of these studies, trying as much as possible to obtain the estimates for the period and quantity reported in each work. The results of all these studies and the homologous estimates from the C-ERA40 dataset are given in Table 1.

Both Wang and Swail's (2002) and our estimates show no statistically significant trends in grid points around the SSLV location nor in the North Atlantic regions considered by Bouws et al. (1996). The estimates from the C-ERA40 data are close to those of Günther et al. (1998) for annual means, 90th and 99th percentile, but fall short of their estimates for the trend on the annual maxima. For the latter quantity our estimates compare well with those of Wang and Swail (2002), but our estimates of trends in the annual mean and 99th percentiles are lower than theirs. Wang and Swail's, Günther's et al. (1998) and our trend estimates are all positive and increase with the percentile considered.

Information on trends of H_S in regions other than the North Atlantic is sparse. Allan and Komar (2000) and Gower et al. (2002) report positive trends off the Northwestern coast of the United States of America. Their estimates are based on buoy measurements of American National Data Buoy Center (NDBC-NOAA) from 1978 to 1999. They report particularly high and statistically significant trends in the measurements of

buoys 46005 and 46002 (offshore the Washington and Oregon states of the USA, respectively), where Gower et al. (2002) report monthly means of 2.1 and 1.9 cm/yr, respectively, and Allan and Komar (2000) report increases in the yearly means of 2.7 and 1.3 cm/yr, respectively. Our C-ERA40 estimates from annual means for the period considered are also statistically significant but lower, of 1 cm/yr at the location of buoy 46005 and 0.9 cm/yr at the location of buoy 46002. Higher trends are found further offshore of the buoy locations.

Table 1. Trend estimates of H_S in the North Atlantic obtained in several studies, including the present one. An asterisk marks trends that were found not to be statistically significant.

Study	Location	Variable	Period	Trend (cm/yr)
Carter and Draper (1998)	Seven Stones light vessel	Annual means	1962-1985	3.4
Bacon and Carter (1991)				2.2
Wang and Swail (2002)	Grid points around SSLV			0.05-0.21*
C-ERA40	Grid points around SSLV			-0.04-0.18*
Bouws et al. (1996)	Box 1 (50°-55°N, 50°-40°W)	Annual 50th percentiles	1961-1987	2.3
Wang and Swail (2002)				-1.0-0.1*
C-ERA40				-0.3-0.4*
Bouws et al. (1996)	Box 2 (50°-55°N, 20°-10°W)	Annual 50th percentiles	1961-1987	2.7
Günther et al. (1998)				1.0
Wang and Swail (2002)				-1.0-0.1*
C-ERA40				-0.3-0.6*
Günther et al. (1998)	Northeast Atlantic	Annual means	1955-1994	0.25-0.75
Wang and Swail (2002)			1958-1997	0.5-2.5
C-ERA40			1958-1997	0.6–1
Günther et al. (1998)	Northeast Atlantic	Annual 90th percentiles	1955-1994	2-3
Wang and Swail (2002)			1958-1997	1-3
C-ERA40			1958-1997	2-3
Günther et al. (1998)	Northeast Atlantic	Annual 99th percentiles	1955-1994	3-4
Wang and Swail (2002)			1958-1997	2-6
C-ERA40			1958-1997	2-4
Günther et al. (1998)	Northeast Atlantic	Annual maxima	1955-1994	7-10
Wang and Swail (2002)			1958-1997	4-7.6
C-ERA40			1958-1997	4-6.7

Sterl et al. (1998) produced the first global reanalysis wave fields by forcing the WAM model on a 1.5º x 1.5º latitude/longitude grid covering the whole globe with the ECMWF ERA-15 reanalysis (Gibson et al 1997) winds from 1979 to 1993. In their study they analyzed the trends in the Hs monthly means and provide maps of trends in the monthly averages of January and July. We have computed homologous trends from the C-ERA40 H_S data set. The global pattern of the trends we obtained is very close to that presented in Sterl et al. (1998). They observed that the highest trends in January were to be found in the northeast North Atlantic and could be as high as 12 cm/yr, and that the

highest trends in July were to the south of Africa and could be as high as 7 cm/yr. Our corresponding estimates from the C-ERA40 dataset are 15 and 7.4 cm/yr, respectively. These high trends in the monthly means are, however, particular to the period considered. Considering the whole C-ERA40 period, 1958-2001, the estimates of trends in these regions fall below 3 cm/yr.

We will now analyse the seasonal trends we have estimated. Figures 2-4 present global maps with the trends in the seasonal mean, 90th and 99th percentiles, respectively, of C-ERA40 H_S data. Regions where the trends are statistically significant at a 5% level are indicated, and the percentages of the global oceans where these trends are significant are also given. The seasons considered are January, February and March (JFM), April, May and June (AMJ), July, August and September (JAS), and October, November and December (OND).

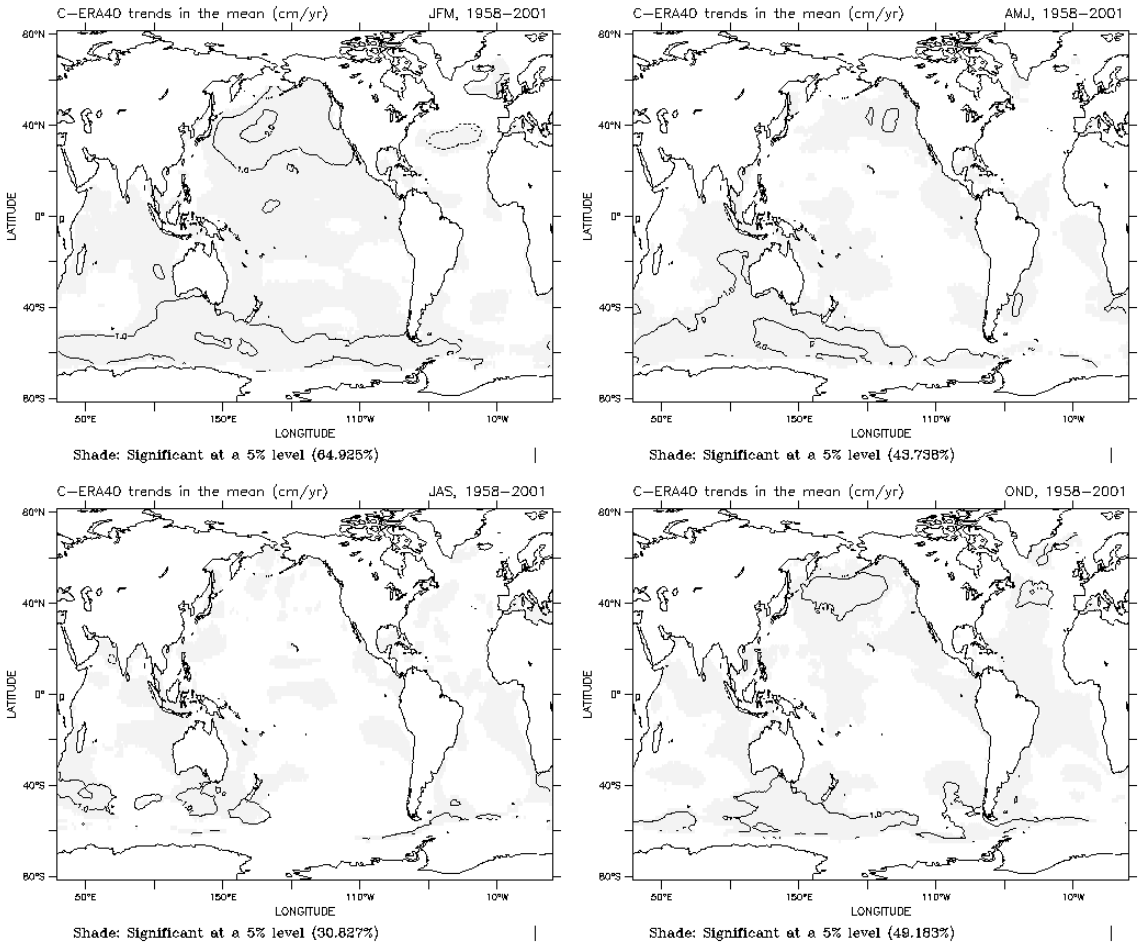

Figure 2. Global changes (cm/yr) in the seasonal mean of C-ERA40 H_S data. The contour interval is 1 cm/yr; contours corresponding to zero are not drawn. Solid and dashed lines represent positive and negative changes, respectively. Shaded areas indicate significant changes at the 5% level.

3.1 SEASONAL MEANS

In the JFM period there are significant trends in almost 65% of the global ocean area. They are particularly high in the North Pacific (up to 2.4 cm/yr), in the Southern Ocean south of Australia and New Zealand (up to 2.1 cm/yr) and in the Northeast Atlantic (up to 2.6 cm/yr). The lowest significant negative trends occur in the mid North Atlantic (as low as –1.5 cm/yr).

In the AMJ period significant positive trends occur only in the Southern Ocean between 60 E and 170W (up to 2.6 cm/yr) and in the Northwest Pacific Ocean (up to 1.2 cm/yr).

JAS is the season where less significant trends occur globally, the highest occurring in the Southern Ocean (up to 2.1 cm/yr).

In the OND period there are mostly positive trends of small amplitude, and these are significant in the Southern Ocean (up to 1.5 cm/yr) North Pacific (up to 1.8 cm/yr) and central North Atlantic (1.3 cm/yr).

Wang and Swail (2004) present trend estimates in the fall and winter seasonal means of H_S from 1958-1997 based on the Cox and Swail (2001) data set for the North Pacific and on the Swail and Cox (2000) data set for the North Atlantic. Their estimates compare with those from presented here as follows:

- In the North Pacific their trends for JFM have a similar pattern to those obtained from the C-ERA40 data set, but their maximal trend (1.8 cm/yr) is lower than that obtained by us. In OND their pattern is also similar to ours: negative and non significant trends in the western North Pacific, positive and significant trends in the central and eastern North Pacific, However, their highest trends are in the eastern North Pacific (up to 1.2 cm/yr), whereas those obtained from the C-ERA40 data set are higher south of the Aleutian Islands (up to 1.8 cm/yr).
- In the North Atlantic the winter trends are again similar to ours in pattern. Wang and Swail (2004) estimate trends that are positive in the northeast (1-3cm/yr, while C-ERA40 gives up to 2.6 cm/yr) and negative at mid latitudes (from -2 to –0.4 cm/yr, while C-ERA40 gives trends as low as -1.5 cm/yr). In the fall the patterns are also similar to ours: mainly a positive pattern centred in the central North Atlantic. Their maximal trend (1.2 cm/yr) is slightly lower than ours (1.3 cm/yr).

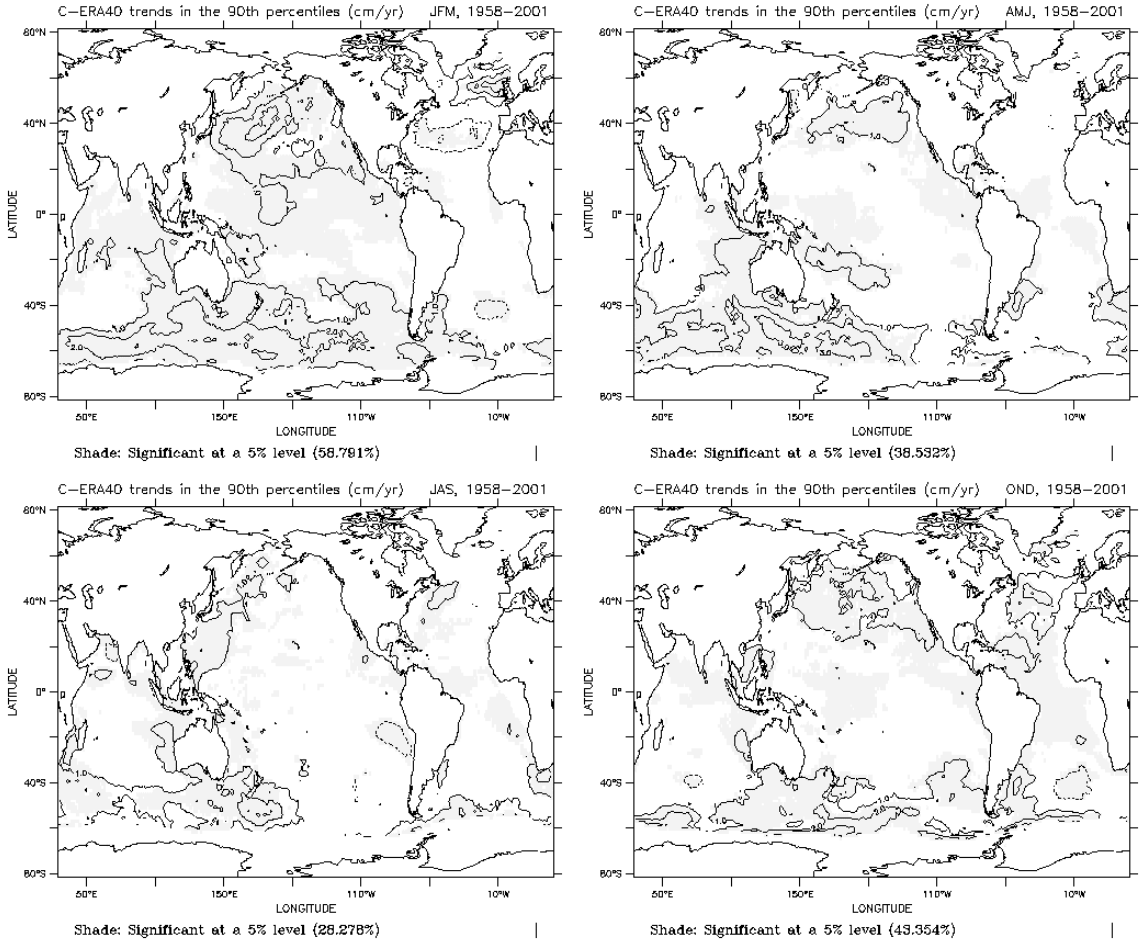

Figure 3. Global changes (cm/yr) in the seasonal 90th percentiles of the C-ERA40 H_S data. The contour interval is 1 cm/yr; corresponding to zero are not drawn. Solid and dashed lines represent positive and negative changes, respectively. Shaded areas indicate significant changes at the 5% level.

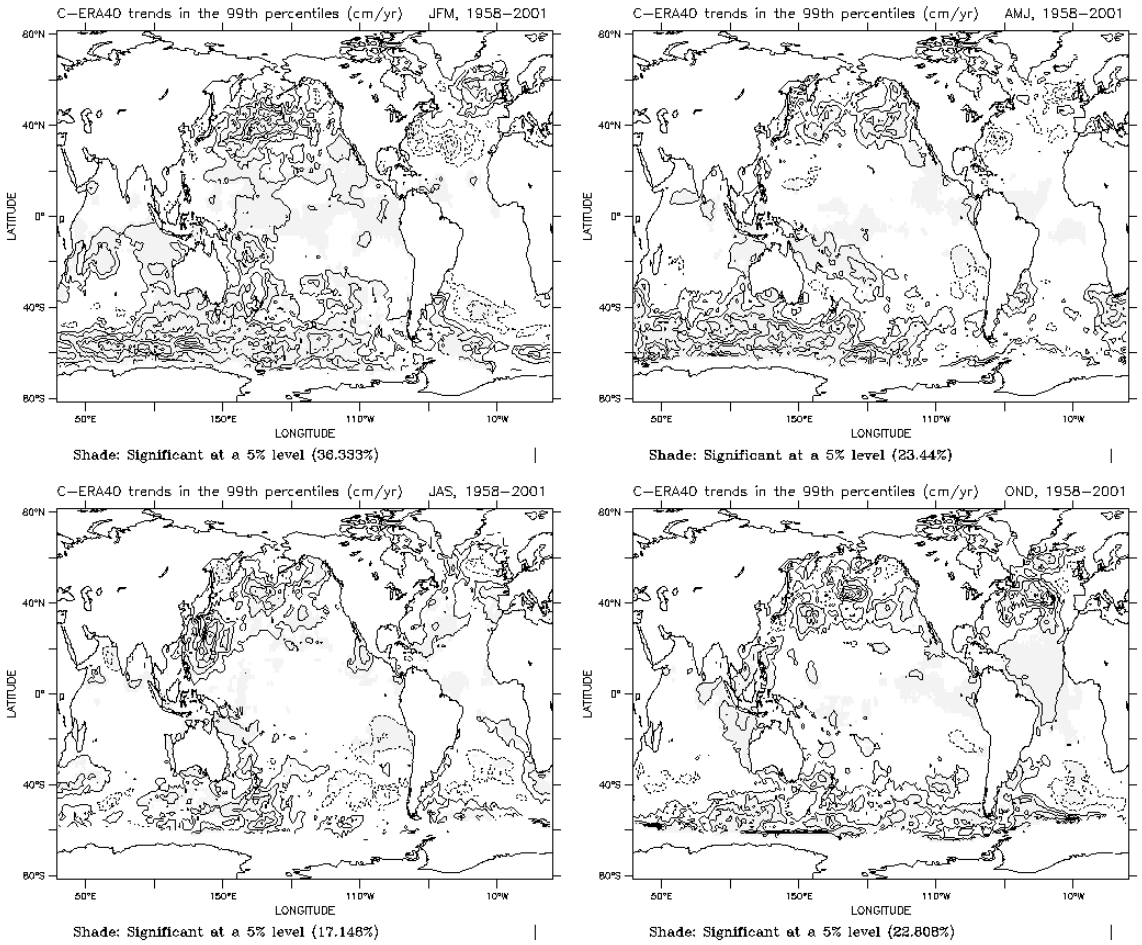

Figure 4. Global changes (cm/yr) in the seasonal 99th percentiles of C-ERA40 H_S data. The contour interval is 1 cm/y; contours corresponding to zero are not drawn. Solid and dashed lines represent positive and negative changes, respectively. Shading indicates areas of significant changes at the 5% level.

3.2 90TH PERCENTILES

The trends in the seasonal 90th percentiles have patterns similar to those of the seasonal means, but the amplitudes are higher and the regions where the trends are statistically significant are smaller, which makes the main features more apparent.

In JFM the highest statistically significant trends are in the North Pacific (up to 3.7 cm/yr), in the Southern Ocean (up to 3.4 cm/yr) and in the Northeast Atlantic (up to 4 cm/yr); the lowest significant trends occur in the mid North Atlantic (as low as –2.1 cm/yr) and southwest of South Africa (as low as –1.7 cm/yr).

In the AMS period the highest positive trends occur only in the Southern Ocean (up to 3.8 cm/yr) and in the west of Argentina (up to 2.4 cm/yr).

As for the seasonal means, JAS is the season when less significant trends occur globally, the highest ones occurring in the Southern Ocean (up to 3.2 cm/yr) and the lowest significant negative trends east of Chile (as low as –1.7 cm/yr) and in the Arabian Sea (as low as –1.9 cm/yr).

In the OND period, as in the case of seasonal means, there are mostly positive trends (up to 5.1 cm/yr south of New Zealand).

Wang and Swail (2002) presented trend estimates in the seasonal 90th percentile of H_S in the North Atlantic for winter, summer and fall from 1958-1997 using the Cox and Swail (2001) and Swail and Cox (2000) data sets. The patterns of the estimates from both data sets are similar, but the trends obtained from the Swail and Cox

(2000) data set have higher amplitudes. The patterns of the trends obtained from the C-ERA40 data set are closer to those obtained from the Swail and Cox (2000). The trend estimates from that data set for summer and fall are also close to ours; however, their winter estimates (6 cm/yr increase in the northeast and –3.5 cm/yr in the subtropics) are higher than those obtained by us.

Wang and Swail (2001) present normalised trends (i.e. as percentages of the 40-year mean) in the North Pacific based on Swail and Cox (2000) data set. Because of the normalization, no quantitative comparisons with our estimates are possible, but the patterns of change are similar to those obtained by us, apart from a significant decrease in the central western North Pacific for the summer data that is not present in our estimates.

3.3 99^{TH} PERCENTILES

We have seen that the trends in the seasonal 90^{th} percentiles have patterns similar to those of the trends in the seasonal means, except that they have higher amplitudes and a smaller region with statistically significant estimates. Analogously, the trends in the seasonal 99^{th} percentiles have patterns similar to those of the 90^{th} percentiles, higher amplitudes (-4.4 to 7.4 cm/yr in JFM, -3.7 to 6.8 cm/yr in AMJ, -3.1 to 6.5 cm/yr in JAS and -3.0 to 8.6 cm/yr in OND), and the regions where the trends are significant are smaller (compare Figures 3 and 4). The increase in the magnitude of the trends and the reduction of the region where they are significant when considering seasonal 99^{th} instead of 90^{th} percentiles is also present in the results of Wang and Swail.

Comparing our estimates with those of Wang and Swail (2001, 2002), most of the comments on the 90^{th} percentiles apply. The estimates of trends in the northeast Atlantic based on the Swail and Cox (2000) dataset are higher than those obtained by us (7.5 cm/yr in their case and 5cm/yr in our case).

4. EXTREME VALUES ANALYSIS

Using the non-stationary GEV model with a linear trend in the scale parameter, Wang and Swail (2004) present differences between the as of 1975 and as of 2000 20-year return value estimates (see Wang and Swail, 2004, Fig. 2 and 6). Both in the non-stationary GEV considered by Wang and Swail (2004) and in the non-homogeneous Poisson process that we consider here, changes in extremes are assumed to be due only to the rate of change of the scale parameter; therefore, when fixing the parameters for a given year in order to estimate return values as for that year, different period returns values (20-, 50-, or 100-year, for instance) will be affected in the same way, by the addition of the same constant. So, instead of presenting the differences between the 20-year return values as of 1975 and 2000 estimated by fixing the estimated model parameters for that year we will just present the rate of change of the location parameter (the difference in the m-year return values, for any m years, in any 25 years period is simply $25\hat{\beta}$).

Figure 5 presents global maps of the estimates of the seasonal trends in the NPP scale parameter obtained from the C-ERA40 H_S data. Regions where the trends are significant at a 5% levels are indicated and the percentages of the global oceans where these trends are significant are also given.

In the JFM period the estimated trends in the scale parameter are significant in almost 59% of the global ocean area. They are particularly high in the Southern Ocean in the region between 50E and 160W (up to 8 cm/yr), in the central North Pacific and Northeast Atlantic. Wang and Swail (2004) show a similar pattern in North Pacific for changes in the 20-year return values as of 1975 and as of 2000, but their changes are higher (250 cm in 25 years, 10 cm/yr) than those obtained by us (7.4 cm/yr). Just as in our case, in the North Atlantic they estimate increases in the northeast (up to 8cm/yr), which are matched by decreases in the mid latitudes.

In the AMF period the trends are mainly positive, in the Southern Ocean of up to 6.6 cm/yr and the north and south-eastern regions of the Pacific of up to 4.7cm/yr.

In the JAS season the most prominent features are increases south of New Zealand (up to 5.3 cm/yr) and southwest of Japan (up to 6.7 cm/yr).

In the OND season positive trends are the most common and prominent feature, and trends are highest in the Southern ocean (up to 5.0 cm/yr), west of Argentina (up to 3.7 cm/yr), west of Canada (up to 3.9 cm/yr) and in the North Pacific (up to 4.8 cm/yr). The patterns of change in the North Atlantic and Pacific are similar to those estimated by Wang and Swail.

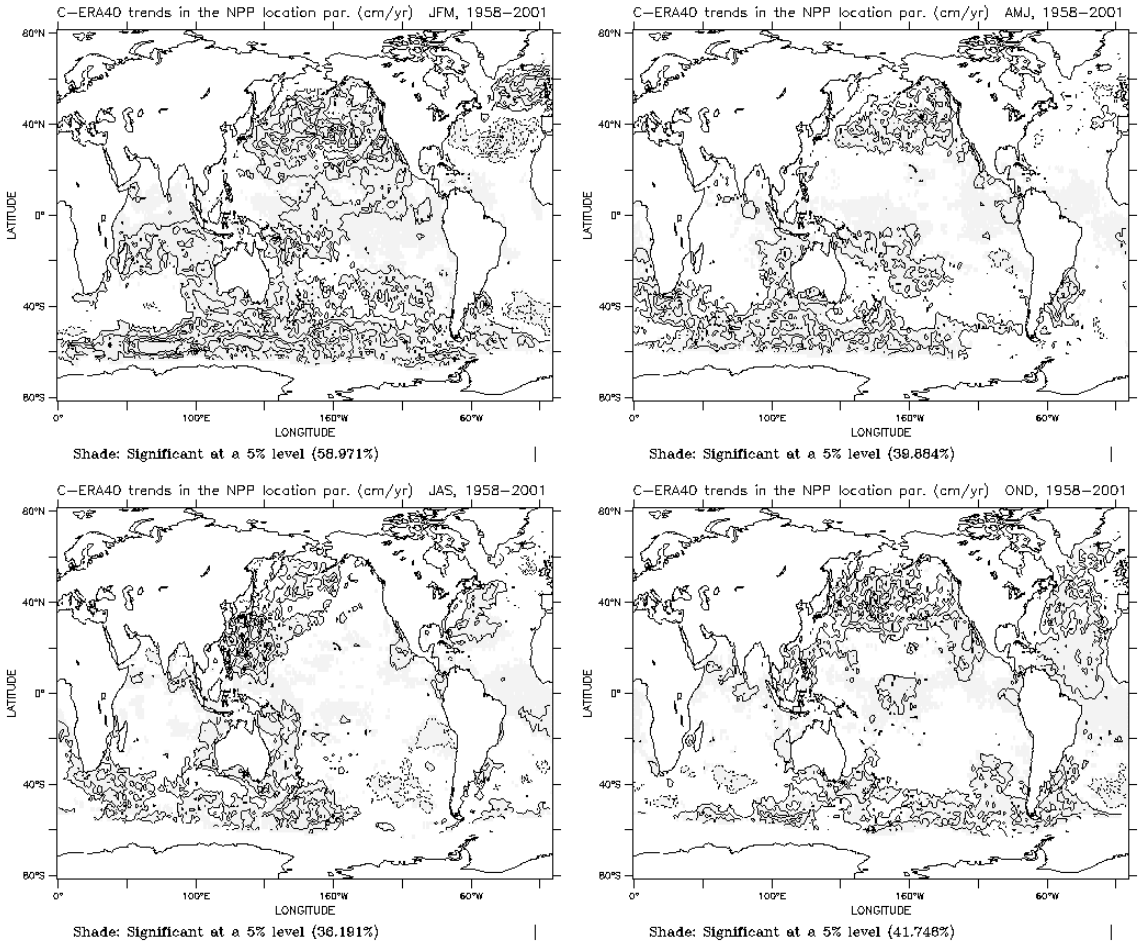

Figure 5. Global changes (cm/yr) in the NPP scale parameter of the C-ERA40 H_S data. The contour interval is 1 cm/yr and zero contours are not drawn. Solid and dashed lines represent positive and negative changes, respectively. Shading indicates areas of significant changes at the 5% level.

5. VARIABILITY MODES

Empirical orthogonal function (EOF) analysis was used to obtain, in each ocean basin, the main modes of variability of the C-ERA40 monthly means, in order to investigate whether they are linked to known dynamic mechanisms (Caires et al, 2004b). It was found that: the most important global EOF, which explains 15% of the global variability, represents swell propagating from the Southern Hemisphere storm track region and its coefficients have a correlation of about 0.80 with the global mean of C-ERA40 H_S. The coefficients of the first EOF coming from the analysis of the North Pacific, which explains 31% of the variability in that basin, has a correlation of about -0.76 with the Pacific-North American Index (PNA, Wallace and Gutzler, 1981). The coefficients of the second EOF coming from the analysis of the North Atlantic, which explains 24% of the variability in that basin, has a correlation of about 0.80 with the North Atlantic Oscillation (NAO, see e.g. Rogers, 1984).

Wang and Swail (2001) used the 99th percentiles of H_S for the JFM period from the Cox and Swail (2001) data set to present estimates of the first EOFs for the North Atlantic and North Pacific and the associated time series of coefficients. For the North Atlantic, their first EOF, which explains 28% of the variability in that basin, has a NAO-like structure and a statistically significant positive trend in its time series of coefficients.

Figure 6 shows the most important EOF spatial pattern of the 99th percentiles for the JFM period in the North Atlantic as obtained from the C-ERA40 H_S data, which explains 29% of the variability in that basin, and the

time series of its coefficients. The structure of the pattern is quite similar to that presented by Wang and Swail, and the coefficients also exhibit a statistically significant trend.

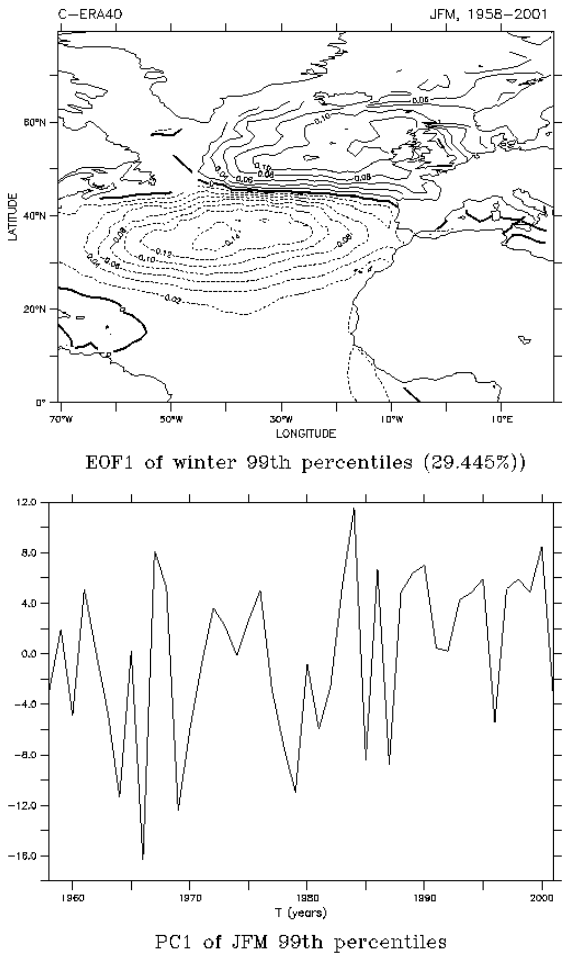

Figure 6. The first mode of the EOF analyses of the 99th percentiles of C-ERA40 H_S data for the JFM period in the North Atlantic.

For the North Pacific the most important EOF obtained by Wang and Swail (2001), which explains 27% of the variability in that basin, has a pattern that resembles the corresponding winter trend pattern, and it is associated with the deepening and eastward extent of the Aleutian low. Its coefficients have a statistically significant positive trend.

As for the North Atlantic, the most important North Pacific EOF and its coefficients explain 32% of the variability in that basin, and have a structure and time variability very similar to that presented in Wang and Swail (2001). The EOF and its time series of coefficients are presented in Figure 7. The time series of coefficients also has a statistically significant trend.

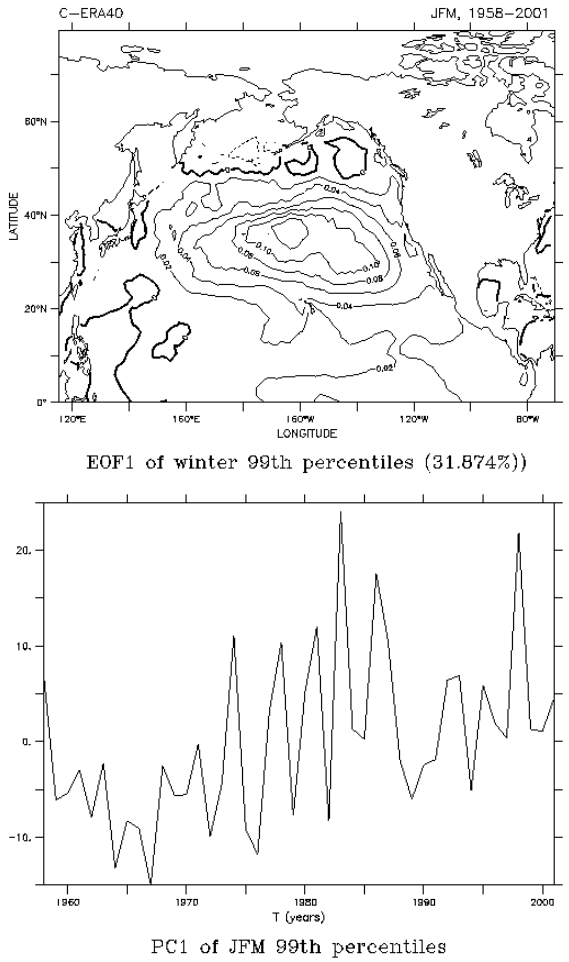

Figure 7. The first mode of the EOF analyses of the 99th percentiles of C-ERA40 H_S data for the JFM period in the North Pacific.

6. CONCLUSIONS

We have presented global estimates of trends in the seasonal means, 90th and 99th percentiles and the NPP location parameters of C-ERA-40 H_S data from 1958 to 2001, and analysed their seasonal variability. We have also given some information about the H_S oceanic main modes of variability.

Regions of the globe with high and statistically significant trends are the central North Pacific, the Southern Ocean and the Northeast Atlantic. Trends in the North Hemisphere are particularly high in the winter and fall; those in the Southern Ocean are high all year round.

Trends of up to 2.6, 5.1, 8.6 are to be expected in the

means, 90th and 99th percentiles, respectively, and the percentage of the global oceans where these trends are statistically significant can be up to 64, 58, and 36%, respectively. JFM is the season where the highest percentages occur and JAS the season where the lowest occur.

The highest trend in the scale parameter is 8 cm/yr, and the percentage of the global oceans where such trend is statistically significant varies seasonally between 36 and 59%.

In terms of variability modes we have the following main conclusions: Variability in the North Atlantic is highly correlated with the NAO, the pattern being of higher waves in the Northeast and lower waves in the mid latitudes. The variability in the North Pacific is correlated with the PNA and with the deepening and eastward extent of the Aleutian low, resulting in positive trends in the central North Pacific. 15% of the global wave variability is due to swell travelling from the Southern Hemisphere storm track region and governs the variability of the global mean.

The trends estimated from the ERA-40 data were compared with those available in the literature, specially with the results of Wang and Swail. ERA-40 trend estimates have magnitudes lower than those given by studies based on observations. The spatial structure of the trends estimated from the C-ERA40 data set is very similar to those of estimates based on wave model results.

The variability modes estimated by Wang and Swail for the North Atlantic and Pacific are very close to those obtained by us. Estimates of trends from the C-ERA40 data compare with those obtained by Wang and Swail as follows:

Compared with estimates based on the Cox and Swail (2001) data set in the North Pacific, the C-ERA-40 estimates of trends in seasonal means are higher, and the patterns of the two differ slightly. No quantitative comparisons were possible for the trends in the seasonal 90th and 99th percentiles, but the spatial patterns are compatible. In terms of trends in scale parameters of the GEV/NPP models, those based on the Cox and Swail (2001) data set are higher, the differences being of 2.5 cm/yr; however, these differences may due to the different approaches used to obtain the estimates. For comparison purposes we have obtained from the C-ERA40 data set estimates of the parameters of the non-stationary GEV model used by Wang and Swail (2004) and observed that the differences between estimates from the 2 approaches (not shown here) can be as high as 3 cm/yr.

The spatial structure of the C-ERA40 estimates is closer to that of the estimates based on the Swail and Cox (2000) data set, but the C-ERA40 trend estimates of seasonal means, 90th and 99th percentiles have lower magnitudes in JFM, with differences in the positive trends of up to 2.5 cm/yr for the 99th percentiles. The estimates of trend in the location parameter of the extreme value distributions are compatible.

REFERENCES

Allan, J. C. and P.D. Komar, 2000: Are ocean wave heights increasing in the eastern North Pacific? *EOS,* **81** (47), 561,566-567.

Anderson, C. W., D. J. T. Carter, and P. D. Cotton, 2001: Wave climate variability and impact on offshore design extremes. Report for Shell International and the Organization of Oil & Gas Producers. 99 pp.

Bacon, S. and D. J. T. Carter, 1993: A connection between mean wave height and atmospheric pressure gradient in the North Atlantic. *Int. J. Climatol*., **13**, 423-436.

Bouws, E., D. Jannink, and G. J. Komen, 1996: The increasing wave height in the North Atlantic Ocean. *Bull. Amer. Meteor. Soc*., **77**, 2275-2277.

Caires, S. and A. Sterl, 2005a: A new non-parametric method to correct model data: Application to significant wave height from the ERA-40 reanalysis. *J. Atmos. Oceanic Tech*. (accepted).

Caires, S. and A. Sterl, 2005b: 100-year return value estimates for ocean wind speed and significant wave height from the ERA-40 data. *J. Clim.* (accepted).

Caires, S., A. Sterl., J.-R. Bidlot, N. Graham, and V. Swail, 2004a: Intercomparison of different wind wave reanalyses. *J. Climate*, **17**, 1893-1913.

Caires, S., A. Sterl, G. Komen, and V. Swail, 2004b: The web-based KNMI/ERA-40 global wave climatology atlas. *Clivar Exchanges*, **30**, 27-29.

Carter, D. J. T. and L. Draper, 1988: Has the North East Atlantic become rougher? *Nature*, **332**, 494.

Coles, S., 2001: *An Introduction to Statistical Modelling of Extreme Values*. Springer Texts in Statistics, Springer-Verlag London.

Cox, A. T. and V. R. Swail, 2001: A global wave hindcast over the period 1958-1997: Validation and climate assessment. *J. Geophys. Res*., **106**,

2313-2329.

Gower, J. F. R., 2002: Temperature, wind, and wave climatologies, and trends from marine meteorological buoys in the Northeast Pacific. *J. Clim*., **15**, 3709-3718.

Günther, H., W. Rosenthal, M. Stawarz, Carretero, J.C., M. Gomez, I. Lozano, O. Serano and M. Reistad, 1998: The wave climate of the Northeast Atlantic over the period 1955-94: the WASA wave hindcast. *Global Atmos. Ocean System*, **6**, 121-163.

Janssen, P.A.E.M., D. Doyle, J. Bidlot, B. Hansen, L. Isaksen and P. Viterbo, 2002: Impact and feedback of ocean waves on the atmosphere. *Advances in Fluid Mechanics*, *Atmosphere-Ocean Interactions*, **I**, WIT press, Ed. W. Perrie. 155-197.

Kalnay, E., M. Kanamitsu, R. Kistler, W. Collins, D. Deaven, L. Gandin, M. Iredell, S. Saha, G. White, J. Woolen, Y. Zhu, M. Chelliah, W. Ebisuzaki, W. Higgins, J. Janowiak, K.C. Mo, C. Ropelewski, J. Wang, A. Leetmaa, R. Reynolds, R. Jenne and D. Joseph, 1996: The NCEP/NCAR 40-year reanalysis project. *Bull. Amer. Meteorol. Soc*., **77**, 437-471.

Kendall, M. G., 1955: *Rank correlation methods*. Charles Griffin.

Komen, G. J., L. Cavaleri, M. Donelan, K. Hasselmann, S. Hasselmann and P. A. E. M. Janssen, 1994:Dynamics and Modelling of Ocean Waves. Cambridge Univ. Press.

Mann, H. B., 1945: Non-parametric tests against trend. *Econometrica*, **13**, 245-259.

Preisendorfer, R. W., 1988: *Principal Component Analysis in Meteorology*. Developments in Atmospheric Sciences, **17**, Elsevier.

Press, W. H., S. A. Flannery, B. P. Teukolsky, and W. T. Vatterling, 1992: *Numerical Recipes in FORTRAN*. Cambridge University Press.

Rogers, J.C., 1984: The association between the North Atlantic Oscillation and the Southern Oscillation in the Northern Hemisphere. *Mon. Wea. Rev.*, **112**, 1999-2015.

Sen, P. K,, 1968: Estimates of the regression coefficient based on Kendall's tau. *J. Amer. Statist. Assoc*., **63**, 1379-1389.

Smith, R. L., 1989: Extreme value analysis of environmental time series: an application to trend detection in ground level ozone(with discussion). *Statist. Sci*., **4**, 367-393.

Sterl, A., G. J. Komen, and P. D. Cotton, 1998: Fifteen years of global wave hindcasts using winds from the European Centre for Medium-Range Weather Forecast reanalysis: Validating the reanalyzed winds and assessing the wave climate. *J. Geophys. Res*., **103**, 5477-5494.

Swail, V. R. and A. T. Cox, 2000: On the use of NCEP-NCAR reanalysis surface marine wind fields for a long-term North Atlantic wave hindcast. *J. Atmos. Oceanic Technol*., **17**, 532-545.

Wallace, J. M. and D. S. Gutzler, 1981: Teleconnections in the geopotential height field during the Northern Hemisphere Winter. *Mon. Wea.Rev*., **109**, 784-812.

Wang, X. L. and V. R. Swail, 2001: Changes of Extreme Wave Heights in Northern Hemisphere Oceans and Related Atmospheric Circulation Regimes. *J. of Climate*, **14**, 2204-2221.

Wang, X. L. and V. R. Swail, 2002: Trends of Atlantic Wave Extremes as Simulated in a 40-Yr Wave Hindcast Using Kinematically Reanalyzed Wind Fields. *J. of Climate*, **15**, 1020-1035.

Wang, X. L. and V. R. Swail, 2004: Historical and possible future changes of wave heights in northern hemisphere oceans. In: *Atmosphere Ocean Interactions*, **2**, W. Perrie (ed.), Wessex Institute of Technology Press, Southampton, UK.